

Benchmarking the HELIOS-2 ENDF/B-VII Library: B&W-1484 and DIMPLE S-06 Criticals

C.A. Wemple

Studsvik Scandpower, Inc.
504 Shoup Ave., Suite 201, Idaho Falls, ID USA
Charles.Wemple@studsvik.com

Keywords: HELIOS-2, benchmarking, ENDF/B-VII, method of characteristics

ABSTRACT

As part of the verification program for the HELIOS-2 code system, examination of the B&W-1484 and DIMPLE S-06 critical experiments was performed. Detailed computation models were developed for both experiments. Core eigenvalues and reaction rates, where available, were compared; after accounting for various biases and uncertainty, the results are generally excellent.

1. INTRODUCTION

The recent development of the HELIOS-2 code¹, with its attendant ENDF-B/VII-based nuclear data library, required an extensive testing and benchmarking effort. In addition to various performance tests, a suite of comparisons to critical experiments and other measurements was included in this effort. The success of such testing provides the requisite level of confidence in results generated by the code for application in reactor analysis.

The HELIOS-2 nuclear data library is based on ENDF/B-VII R0 evaluated data files², the most comprehensive evaluations available. The main cross section processing was performed using the NJOY code³, version 99.161. Several modifications were made to this code, including the addition of a module that uses NJOY-generated data to build the resonance integral data required for the HELIOS-2 library format. The new library contains neutron data for 360 materials, including 171 fission products and 44 actinides, with 100 resonance materials. The upper limit of the resonance region was increased from 9.119keV to 111.1keV. Photon cross section data are available for 356 materials. The base nuclear data library uses 177 neutron groups and 48 photon groups; a production library with 49 neutron groups and 18 photon groups is also available.

2. THE CRITICAL EXPERIMENTS

2.1 B&W-1484 Criticals

This series of fifteen critical experiments⁴ (ICSBEP, LEU-COMP-THERM-011) was conducted at Babcock and Wilcox's CX-10 critical facility in the late 1970s. The experiments used individual aluminum-clad uranium dioxide fuel pins in a square lattice.

Thirteen of the fifteen configurations (Cores III-IX) were designed to simulate PWR-type fuel bundle storage racks, with fuel pins arranged in 14x14 square clusters with variable spacing between the clusters; boron carbide absorber rods were placed in the inter-cluster gaps for five of these configurations. Two of the fifteen configurations (Cores I and II), the most commonly cited of the series, were arranged in a single, roughly circular array and a single square array, respectively. The uranium enrichment in all fuel pins was 2.5% ^{235}U , with either ordinary or borated water used as the moderator and reflector. The pin pitch was 1.636cm for all configurations. The moderator height and boron concentration in the moderator were used to control criticality; Cores I and IX were unborated. Only criticality was measured in these configurations; no reaction rate data were gathered.

This series of criticals is particularly useful for code benchmarking, as it provides a scenario where accurate calculation of the leakage is crucial to achieving good comparisons with the critical experiments. This is especially true for the first configuration, which has a small, tightly packed core.

2.2 DIMPLE S-06 Criticals

A series of four critical experiments⁵ (ICSBEP, LEU-COMP-THERM-055; IRPhEP, DIMPLE-LWR-EXP-02) was conducted at AEA Technology's Winfrith site during the late 1980s and early 1990s. These experiments were designed to simulate the peripheral regions of a PWR and modeled the equivalent of twelve 16x16 PWR fuel bundles, arranged in a cruciform array. The first configuration (S-06A) represented the relevant twelve bundles with a water reflector; the second configuration (S-06B) added a stainless-steel baffle around the cluster of assemblies, with a surrounding water reflector. The other configurations were considerably more complicated and of lesser relevance for benchmarking, and consequently are not included in this work. The fuel pins were uranium dioxide, enriched to 3% in ^{235}U , with stainless steel clad. Ordinary water was used for the reflector and moderator. The pin pitch for both configurations was 1.2507cm. Criticality was achieved by variation of the moderator level only. Reaction rates (^{235}U fission, ^{239}Pu fission, ^{238}U fission and capture) were measured on several radial traces along the primary axes and assembly-level diagonals for both configurations.

These two criticals also provide a test of the leakage calculation. In addition, the second configuration provides a rare opportunity for code developers to characterize solution accuracy for a PWR baffle, an important issue for power reactor modeling.

3. THE MODELS

3.1 The HELIOS-2 Code

The HELIOS-2 code system is a general-geometry, two-dimensional, coupled neutron-gamma, current-coupled transport code designed to perform lattice calculations on various reactor configurations. The transport solution may be performed by either the collision probability (CP) method or the method of characteristics (MoC). Current coupling between structures is accomplished via arbitrary-order angular coupling

definitions pre-programmed into the code and selected by user input; explicit (true) region coupling may also be selected. Angular integration is performed via selection of a quadrature. In the CP solution, the polar angle integration is performed explicitly during the computation of the response fluxes and only the azimuthal angle requires numerical integration. For the MoC solution, numerical integration is performed for both the polar and azimuthal domains; several polar angle quadrature sets⁶⁻⁸ are available in the code for this purpose. Boundary conditions are modeled by either a reflective (specular) boundary or a general albedo matrix. The code has a general burnup and decay capability with restart, a macro-oriented input scheme, and comes packaged with powerful pre-and post-processing codes (AURORA and ZENITH), a graphical geometry visualization tool (ORION), a hierarchical database subroutine package (HERMES), and various multi-group cross section libraries based on ENDF/B-VI and JEF-2.2. The resonance cross section calculation uses the subgroup method; interference effects between isotopes may be included in the calculation, along with an explicit Dancoff calculation.

All calculations performed for this paper used the new MoC solver with explicit region coupling ($k=0$) and the 177-group neutron cross section library. The optimal quadrature set of Yamamoto⁷ with two polar angles was used for the polar integrations.

3.2 HELIOS-2 Computational Models

Detailed, one-eighth core models of the B&W-1484 criticals were constructed with the HELIOS-2 code for Core I (circular), Core II (simple square), Cores IIIA-G (small inter-cluster spacing), and Core IX (large inter-cluster spacing). For the Core I model, the maximum and minimum ray spacings were set to 0.2mm and 0.005mm, respectively, and 48 angles were used per half-space to improve the flux solution resolution; all other cases used 0.25mm maximum spacing and 24 angles per half-space. Figures 2-5 show the core layouts for Cores I, II, III, and IX, respectively⁹; Figure 5 shows a close-up of the pin-cell geometric representation in the HELIOS-2 model.

Detailed, one-fourth core models of the DIMPLE S-06 criticals were constructed for configurations S-06A (water reflected) and S-06B (steel baffle + reflector). The maximum ray spacing was set to 0.25mm and 24 angles were used per half-space. Figure 6 shows a close-up of the pin-cell geometric representation in the HELIOS-2 model; Figures 7 and 8 show the core layouts for Core S-06A and S-06B, respectively¹⁰.

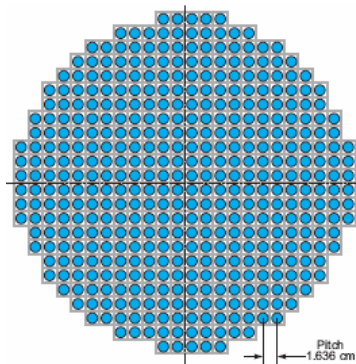


Fig. 1 Core I layout.

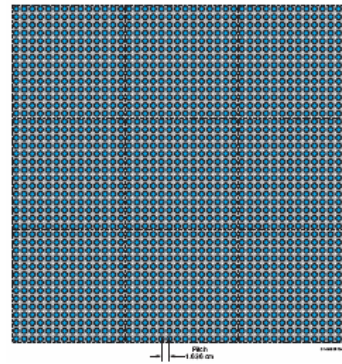


Fig. 2 Core II layout.

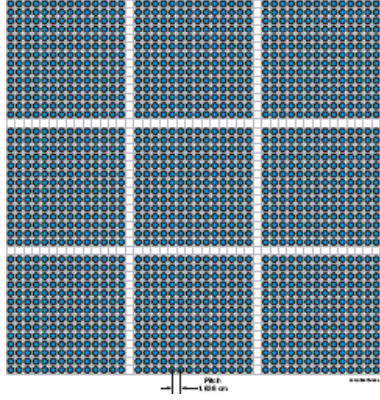


Fig. 3 Core III layout.

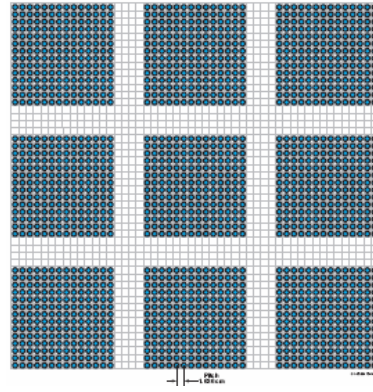


Fig. 4 Core IX layout.

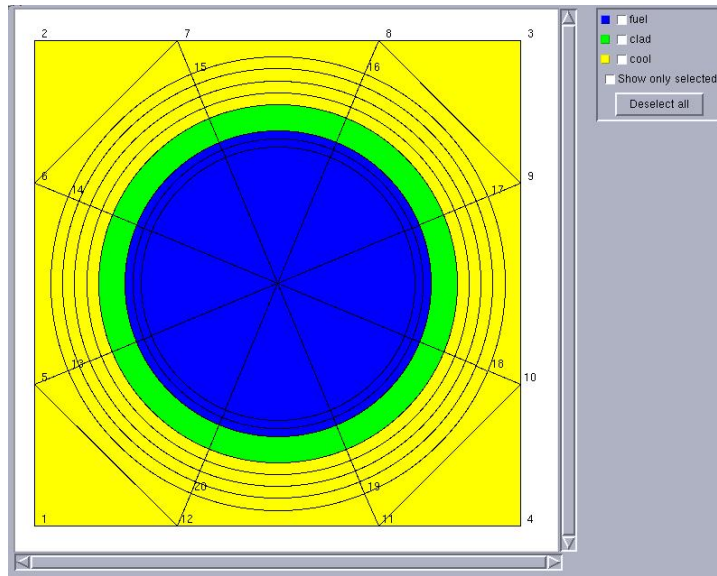


Fig. 5 HELIOS-2 pin-cell geometric representation used for the B&W-1484 criticals.

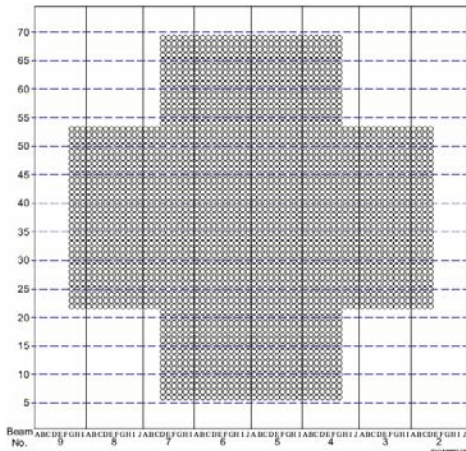


Fig. 6 DIMPLE S-06A layout.

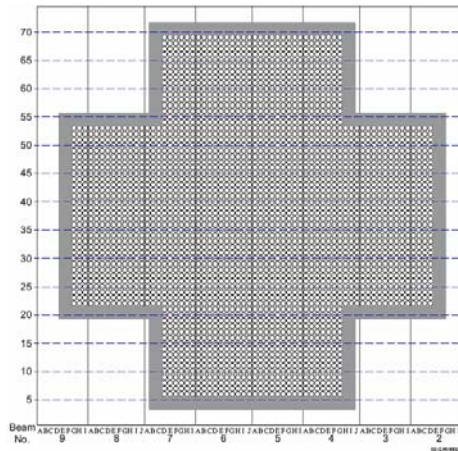


Fig. 7 DIMPLE S-06B layout.

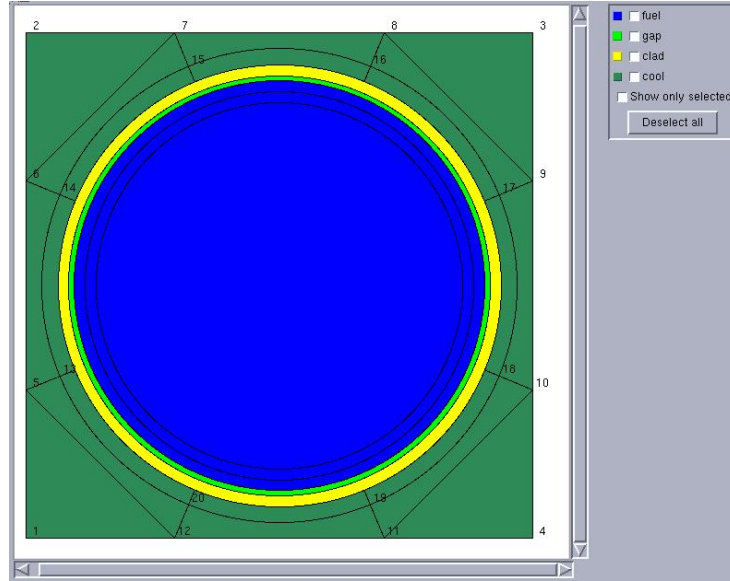


Fig. 8 HELIOS-2 pin-cell geometric representation used for the DIMPLE criticals.

4. RESULTS

4.1 B&W-1484

The HELIOS-2 calculation results for the B&W-1484 criticals are summarized in Table 1. The differences are computed on the basis of the benchmark eigenvalues and uncertainties, which are taken from the ICSBEP benchmark specification⁹. Bucklings for all cases were computed from the specified critical moderator heights with an extrapolation length of 7.79cm; this value was extracted from the historical buckling value used for Core I ($4.1 \times 10^{-4} \text{ m}^{-2}$). The results are generally quite good; all but one case is within 2σ of the benchmark value.

Table 1 HELIOS-2 core eigenvalue results for the B&W-1484 criticals.

Case	HELIOS-2	Benchmark	Uncert. (pcm)	Delta-k (pcm)	# Std. Dev.
Core I	0.99831	1.0010	180	-269	-1.49
Core II	0.99634	1.0009	320	-456	-1.42
Core IIIa	0.99809	1.0009	320	-281	-0.88
Core IIIb	0.99889	1.0009	320	-201	-0.63
Core IIIc	0.99849	1.0009	320	-241	-0.75
Core IIId	0.99564	1.0009	320	-526	-1.64
Core IIIe	0.99546	1.0009	320	-544	-1.70
Core IIIf	0.99554	1.0009	320	-536	-1.67
Core IIIg	0.99447	1.0009	320	-643	-2.01
Core IX	1.00406	1.0010	180	306	1.70

The Core III results (Table 2), which differ only by critical moderator height and boron concentration, can be examined for dependencies on these parameters. Plotting the trends, as shown in Figures 9, provides little evidence for any obvious correlations. In fact, there seem to be three clusters of results: one above 760ppm or 140cm; a second between 720 and 760ppm or 110 and 140cm; and a third below 720ppm or 110cm. The spread between high and low eigenvalues is approximately 450pcm and the maximum Δk is 643pcm.

Table 2 HELIOS-2 core eigenvalues for B&W Core III, showing variation with boron concentration and critical moderator height.

Case	HELIOS-2	Boron (ppm)	Buckling	Crit. Ht. (cm)	Δp (pcm)	HELIOS-2 + bias
Core IIIa	0.99809	769	3.87E-04	148.63	-7	0.99802
Core IIIb	0.99889	764	4.06E-04	144.88	0	0.99889
Core IIIc	0.99849	762	4.31E-04	140.38	11	0.99860
Core III d	0.99564	753	4.87E-04	131.32	37	0.99601
Core IIIe	0.99546	739	5.69E-04	120.64	63	0.99608
Core III f	0.99554	721	6.73E-04	110.04	117	0.99670
Core III g	0.99447	702	7.96E-04	100.32	172	0.99617

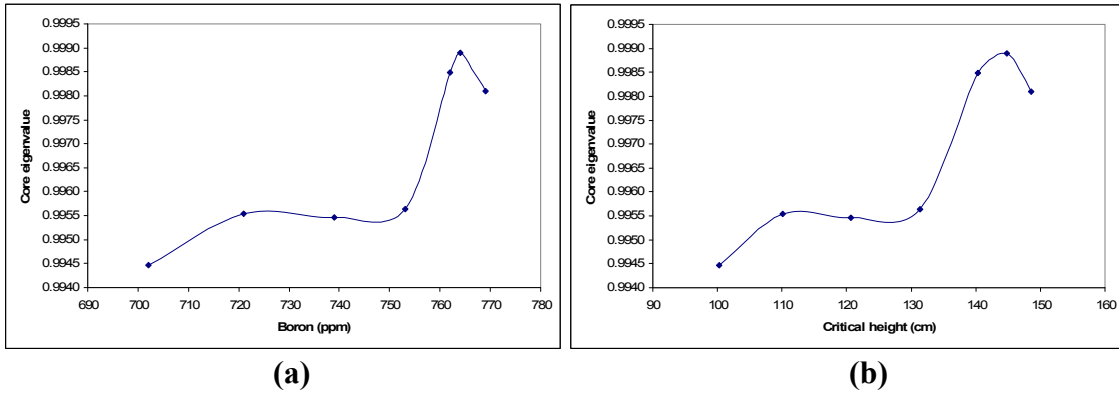


Fig. 9 Core eigenvalue variation with boron concentration (a) and critical moderator height (b).

The original experiment report⁴ (Fig. 26) defines a bias in the calculations from the moderator height variation. Application of this bias produces modified results, shown in Table 2; this reduces the spread to approximately 280pcm and the maximum Δk to 489pcm, a significant improvement in the calculation results. The variation with moderator height is shown in Figure 10 and shows significantly improved behavior, i.e., closer to a horizontal line.

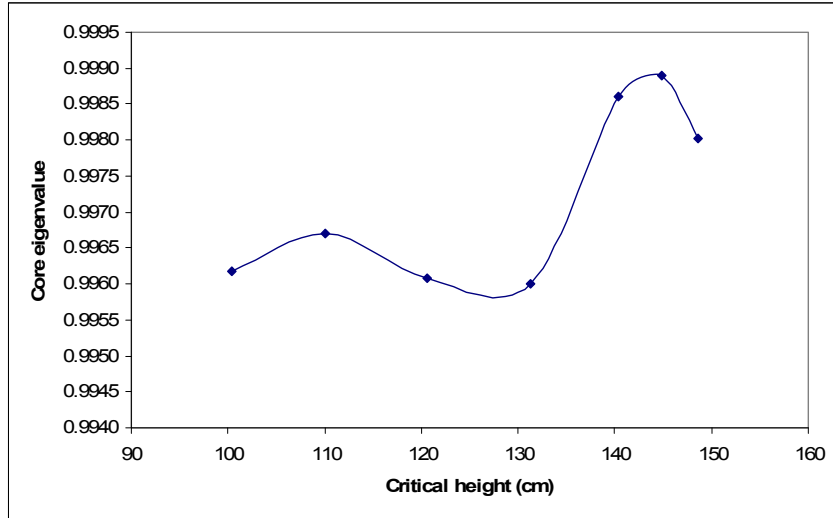


Fig. 10 Modified core eigenvalue variation with critical height.

4.2 DIMPLE S-06

The HELIOS-2 calculation results for the DIMPLE S-06 criticals are summarized in Table 1. The differences are computed on the basis of the benchmark eigenvalues and uncertainties, which are taken from the ICSBEP benchmark specification¹⁰. Axial buckling values were taken from the IRPhEP benchmark specification¹¹. The results display excellent agreement, with both configurations within 200pcm of the benchmark eigenvalues.

Table 4 HELIOS-2 core eigenvalue results for DIMPLE S-06 criticals.

Case	HELIOS-2	Benchmark	Uncert. (pcm)	Delta-k (pcm)
S-06 A	1.00188	1.0000	250	188
S-06 B	0.99899	1.0000	250	-101

Selected reaction rate comparisons (²³⁵U and ²³⁸U fission) are shown in Appendix A, Tables A.1 – A.4. These particular reactions were chosen to characterize the thermal and fast flux calculation accuracy, respectively; the other primarily thermal reactions (²³⁹Pu fission and ²³⁵U capture) display behavior similar to the ²³⁵U fission. Tables A.5 and A.6 provide the measured relative reaction rates for the selected reactions in configuration S-06A, normalized to the value at the indicated location. Reaction rates in the core interior show excellent results, with the errors increasing towards the core periphery. The presence of the baffle ameliorates this somewhat, with better behavior near the periphery. This behavior suggests some inaccuracy in computing the radial leakage, especially for the reflected core; other benchmark calculations performed during the HELIOS-2 verification suggest that this may be solved by a finer meshing of the core and inner reflector. However, these calculations are approaching the code memory

limits. Future code revisions should improve this aspect of HELIOS-2 performance and permit enhanced meshing for this benchmark.

5. CONCLUSIONS

Detailed models of the B&W-1484 and DIMPLE S-06 criticals were created with the HELIOS-2 code. Calculated core eigenvalue results for both experiments showed excellent agreement with measurements. For DIMPLE, comparisons with measured reaction rates showed excellent agreement in the core interior, with somewhat less accurate reproduction of measured values near the core periphery. Future improvements in the code, specifically those to improve memory utilization, should allow the necessary refinement in the spatial meshing to achieve even more accurate results.

ACKNOWLEDGMENTS

The author would like to acknowledge Nicholas Gheorghiu of Studsvik Scandpower for his work developing the HELIOS-2 ENDF/B-VII nuclear data library, and the late Rudi Stamm'ler for numerous technical discussions, his friendship, and his years of dedication to the HELIOS code.

REFERENCES

1. C.A. WEMPLE, H-N.M. GHEORGHIU, R.J.J. STAMM'LER, and E.A. VILLARINO, "Recent Advances in the HELIOS-2 Lattice Physics Code," *Proceedings of the International Conference on the Physics of Reactors (PHYSOR 2008)*, Interlaken, Switzerland (2008).
2. M.B. CHADWICK, et al., "ENDF/B-VII.0: Next Generation Evaluated Nuclear Data Library for Nuclear Science and Technology," *Nuclear Data Sheets* **107**, 2931 (2006).
3. R.E. MACFARLANE and D.W. MUIR, "The NJOY Nuclear Data Processing System, Version 91," LA-12740-M, Los Alamos National Laboratory (1994).
4. M.N. BALDWIN, G.S. HOOVLER, R.L. ENG, and F.G. WELFARE, "Critical Experiments Supporting Close Proximity Water Storage of Power Reactor Fuel," BAW-1484-7 (1979).
5. A.D. KNIPE, B.M. FRANKLIN, B.L.H. BURBIDGE, M.F. MURPHY, A.S. DAVIES, and D. HANLON, "The DIMPLE Cruciform Assembly Benchmark Series," AEA-RS-1072 (1981).
6. A. LEONARD and C.T. MCDANIEL, "Optimum Polar Angles and Weights," *Trans. Am. Nucl. Soc.* **73**, 171 (1995).
7. A. YAMAMOTO, M. TABUCHI, N. SUGIMURA, T. USHIO, and M. MORI, "Derivation of Optimal Polar Angle Quadrature Set for the Method of Characteristics Based on Approximation Error for the Bickley Function," *Nucl. Sci. Tech.*, **44** (2), 129-136 (2007).

8. J.Y. CHO and H.G. JOO, "Solution of the C5G7MOX benchmark three-dimensional extension problems by the DeCART direct whole core calculation code," *Prog. Nucl. Ener.*, **48**, 456-466 (2006).
9. LEU-COMP-THERM-011, International Handbook of Evaluated Criticality Safety Benchmark Experiments (2008).
10. LEU-COMP-THERM-055, International Handbook of Evaluated Criticality Safety Benchmark Experiments (2008).
11. DIMPLE-LWR-EXP-002, International Handbook of Evaluated Reactor Physics Benchmark Experiments, NEA/NSC/DOC(2006)1 (2008).

